Eur. Phys. J. AP **6**, 101–108 (1999)

THE EUROPEAN PHYSICAL JOURNAL APPLIED PHYSICS

Random pseudo promptings applied to the thermal characterization of a wet porous material

E. Delacre[a], D. Defer, E. Antczak, and B. Duthoit

Laboratoire d'Artois de Mécanique et Habitat, Équipe thermique instrumentation, Université d'Artois, Faculté des Sciences Appliquées, 62400 Béthune, France

Received: 24 July 1998 / Revised and accepted: 21 December 1998

Abstract. The generalized impedances allow to characterize a one-way thermal system whose two faces are accessible. From experimental measurements of the flux densities and variations in temperature in the access faces of a homogeneous material, the two generalized impedances of storage and transfer are calculated in the frequential field. The theory of the thermal quadripole enables to determine a theoretical expression of these impedances. After a sensitivity study which underlines the accessible parameters and the optimal frequency band, an optimization procedure of the setting of the ideal model of one of the two impedances on the corresponding experimental curve allows to identify the effusivity and the thermal diffusivity of material. The method is applied to the study of a sand with three water contents.

PACS. 67.80.Gb Thermal properties – 06.20.-f Metrology – 81.05.Rm Porous materials; granular materials

Nomenclature

a	Thermal diffusivity ($m^2\,s^{-1}$)
b	Thermal effusivity ($J\,K^{-1}\,m^{-2}\,s^{-1/2}$)
c	Specific heat capacity ($J\,kg^{-1}\,K^{-1}$)
C_{xx}	Autocorrelation function
C_{xy}	Cross-correlation function
$C_{\mathrm{f}i}$	Fluxmeter capacity i ($J\,K^{-1}\,m^{-2}$)
f	Frequency (Hz)
FT	Fourier's operator
H	Transfer function ($W\,m^{-2}\,K^{-1}$)
H_1, H_2, H_3	Characteristic functions ($W\,m^{-2}\,K^{-1}$)
ℓ	Thickness (m)
r	Ratio of $R_{\mathrm{c}i}/R_{\mathrm{f}i}$
R_{ci}	Contact resistance i ($K\,m^2\,W^{-1}$)
$R_{\mathrm{f}i}$	Fluxmeter thermal resistance i ($K\,m^2\,W^{-1}$)
S_{xx}	Power spectral density
S_{xy}	Cross spectral density
t	Time (s)

Greek symbols

θ	Temperature (K, °C)
$\Sigma\theta, \Delta\theta$	Generalized magnitudes of temperature (K)
λ	Conductivity ($W\,m^{-1}\,K^{-1}$)
ρ	Density ($kg\,m^{-3}$)
ϕ	Flux density ($W\,m^{-2}$)
$\Sigma\varphi, \Delta\varphi$	Generalized magnitudes of flow ($W\,m^{-2}$)
χ^2	Merit function
ω	Pulsation ($rad\,s^{-1}$)

1 Introduction

A wet porous material constitutes a complex thermal system including several phases. Its total thermal characterization implies to define apparent quantities. If the density is known or easily accessible, the thermal characterization of the system amounts to determining a couple of characteristic quantities. This can be the apparent conductivity and the specific heat or the diffusivity and the effusivity. Many methods of measurements do exist [1,2,12], however the wet material pose a specific problem. This one results from the nonstationary and nonlinear character of the studied system. Indeed, any method of measurement implies a thermal excitation of the medium from

[a] e-mail: defer@univ-artois.fr

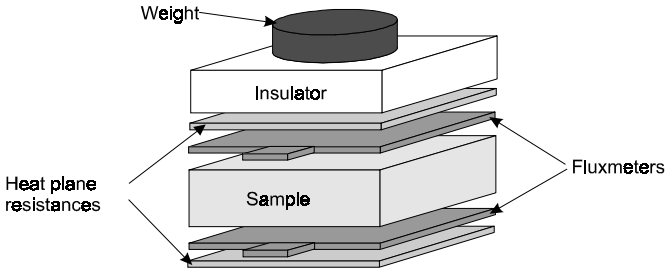

Fig. 1. Experimental device.

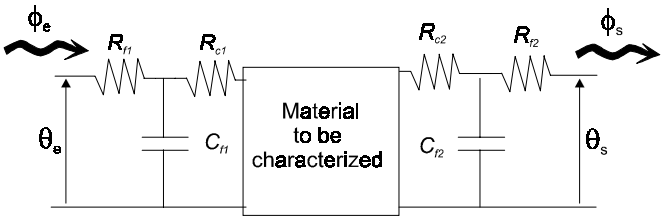

Fig. 2. Schema of the electric analogy.

which a hydrous imbalance and mass transfers can result. The obtained results can then depend on the method used and the energy dissipated in material for the characterization [3].

The remarkable character of the random pseudo binary signal (SBPA) is to use a very low amplitude signal test, which minimizes the disturbance of the medium. This signal could be applied to a balanced system or could come to superimpose itself on other existing solicitations. This method is thus classically employed in electronics or in mechanics to identify nonstationary systems in the process of operation [11]. The developed approach results in being located in the frequential field. The random pseudo binary signal has a fundamental property related to its autocorrelation function, which appears as a periodic series of triangles. The base width of these triangles is all the more small since the rate of clock controlling the generation of the signal is fast. These functions tend towards Dirac's impulses and thus guarantee good richness of spectrums of the thermal signals. SBPA is largely used in the procedures of identification of the systems taking into account the excellent compromise which it achieves between the richness of spectrum and the minimum capacity injected into the medium.

The spectral densities are obtained from measurements of flows and temperatures. The transfer functions are calculated. From these functions, the parameters required are identified simultaneously by an inverse procedure. That implies a sensitivity study to the transfer function parameters, and the characteristic parameters are then determined by an iterative optimization method. The disturbances generated by the sensors are not neglected, they are modelled by the resistances and localized capacities introduced into the model. These quantities, considered unknown, are integrated in the sensitivity study and result in increasing the number of parameters to be identified.

2 Theoretical aspects

2.1 Spectral densities and transfer functions

The studied system is subjected to unidirectional exchanges. The experimental device is represented Figure 1.

The parallelepipedic plate-shaped sample, is placed between two sensors of flow and temperature [4]. In order to check the unidirectionality property of the evolutions, transverse dimensions are selected sufficiently large in front of the thickness (8 cm) so that the system can be regarded as being unidirectional in the central zone of the system where measurement is carried out. This thickness is also chosen such as being lower than twice the characteristic thickness that squares with the attenuation of the signal. Heating resistances are laid out on the external face of each fluxmeter. This device leads to the modeled thermal system starting from an electric analogy which is presented Figure 2.

Each sensor is combined with a resistance and a capacity ($R_{\mathrm{f1}}, C_{\mathrm{f1}}$; $R_{\mathrm{f2}}, C_{\mathrm{f2}}$). The imperfect contact between the sample and the sensor introduces additional resistances (R_{c1}; R_{c2}) [10] to the interface. The whole made up in this way, seems a multilayer conductive system. The well-known formalism of the thermal quadripole [5,6] leads, in the frequential field, to an input/output relation of the following type:

$$\begin{bmatrix}\theta_1\\ \varphi_1\end{bmatrix} = \begin{bmatrix}E & G\\ H & F\end{bmatrix}\begin{bmatrix}\theta_n\\ \varphi_n\end{bmatrix}. \tag{1}$$

By introducing the generalized magnitudes of flow and temperature defined from the combinations of the following temporal evolutions

$$\begin{cases}\Sigma\varphi(t) = \varphi_1(t) + \varphi_2(t)\\ \Sigma\theta(t) = \theta_1(t) + \theta_2(t)\\ \Delta\varphi(t) = \varphi_1(t) - \varphi_2(t)\\ \Delta\theta(t) = \theta_1(t) - \theta_2(t)\end{cases} \tag{2}$$

and by combination of (1) and (2) in the frequential field, we obtain the following relations:

$$\begin{cases}\Sigma\varphi(f) = H_1\Delta\theta(f) + H_2\Sigma\theta(f)\\ \Delta\varphi(f) = H_2\Delta\theta(f) + H_3\Sigma\theta(f)\end{cases} \tag{3}$$

where

$$H_1 = \frac{1 + (E+F)/2}{G}$$
$$H_2 = \frac{F-E}{2G}$$
$$H_3 = \frac{-1 + (E+F)/2}{G}.$$

It appears that a multilayer system is entirely characterized by three generalized transfer functions, H_1 conveying the heat transfer through the system, and H_3 the heat storage within the medium. As for H_2, it characterizes

the structure space dissymmetry and indicates that the ways of transfer and storage are coupled in the case of a dissymmetrical system. In our study, the system to be characterized is a homogeneous material on a macroscopic scale, thus symmetrical. The only cause of possible dissymmetry lies in a possible difference of the disturbances due to the metrology on both sides of material. Theoretical simulations of the transfer functions show that at the approached work frequencies (lower than 10^{-1} Hz), the possible effects generated by differences of the parameters related to metrology on the functions H_1 and H_3 are negligible. In the considered applications, the function H_2 remains very slight in front of the two other functions, and could be neglected during the estimate of H_1 and H_3. According to these remarks and in order to simplify, the system will be considered symmetrical by admitting that contact resistances are equal in plans 1 and 2, since the sensors are identical. The H_2 function is then equal to zero and the system is characterized by a diagonal transfer matrix:

$$\begin{bmatrix} \Sigma\varphi(f) \\ \Delta\varphi(f) \end{bmatrix} = \begin{bmatrix} H_1 & 0 \\ 0 & H_3 \end{bmatrix} \begin{bmatrix} \Delta\theta(f) \\ \Sigma\theta(f) \end{bmatrix}. \tag{4}$$

The random signals processing classically results in expressing relations of statistical dependencies between quantities. This process results in introducing into the temporal field correlation functions, and in considering the signals spectral densities in the frequential field.

Four correlation functions are defined. These are the autocorrelation functions of the variation of the temperatures and of the sum of the temperatures $C_{\Delta\theta\Delta\theta}$ and $C_{\Sigma\theta\Sigma\theta}$, and the flow-temperature cross-correlation functions $C_{\Delta\theta\Sigma\varphi}$ and $C_{\Sigma\theta\Delta\varphi}$. According to the theorem of Wiener-Kinchine, the spectral densities are the Fourier transforms of these functions [7].

The power spectral densities are defined by:

$$\begin{cases} S_{\Delta\theta\Delta\theta}(f) = \mathrm{FT}[C_{\Delta\theta\Delta\theta}(\tau)] \\ S_{\Sigma\theta\Sigma\theta}(f) = \mathrm{FT}[C_{\Sigma\theta\Sigma\theta}(\tau)] \end{cases} \tag{5}$$

and the cross spectral densities will be:

$$\begin{cases} S_{\Delta\theta\Sigma\varphi}(f) = \mathrm{FT}[C_{\Delta\theta\Sigma\varphi}(\tau)] \\ S_{\Sigma\theta\Delta\varphi}(f) = \mathrm{FT}[C_{\Sigma\theta\Delta\varphi}(\tau)] \end{cases}. \tag{6}$$

And then the Fourier transforms of the impulse responses of the system seem to be the ratio of the spectral densities:

$$\begin{cases} H_1(f) = \dfrac{S_{\Delta\theta\Sigma\varphi}(f)}{S_{\Delta\theta\Delta\theta}(f)} \\ H_3(f) = \dfrac{S_{\Sigma\theta\Delta\varphi}(f)}{S_{\Sigma\theta\Sigma\theta}(f)} \end{cases}. \tag{7}$$

The imposed solicitations are random pseudo binary signals (SBPA). These signals generate correlation functions characterized by series of impulses which guarantee good richness of spectrum. However, in practice, one never has a white noise and the solicitations are obtained in a finite spectral band. Within this band, certain frequencies are not excited enough to lead to reliable information. Exploitable information is detected by using the coherence function $\Gamma(f)$. For a couple of spectral densities $S_{xx}(f)$ and $S_{xy}(f)$, the coherence function is defined by [13]:

$$\Gamma(f) = \frac{|S_{xy}(f)|^2}{S_{xx}(f)S_{xx}(f)}. \tag{8}$$

When signals x and y are perfectly correlated, the function $\Gamma(f)$ which takes real values ranging between 0 and 1, tends towards 1. The coherence function makes it possible to know the quality of information obtained and to draw aside the non significant data.

2.2 Sensitivity study, identification by optimization

The H_1 and H_3 functions globally characterize the considered system in the frequential field. For the symmetrical multilayer system that we consider, they depend on six variables. On the one hand the characteristics of material, the effusivity b, the diffusivity a and the thickness ℓ, and on the other hand the parameters related to metrology, *i.e,* the contact resistance r, sensors resistance $R_{\mathrm{f}i}$ as well as their capacity $C_{\mathrm{f}i}$. The effusivity and the thermal diffusivity of material constitute here the required final quantities. In this study, optimizations are carried out on the two functions H_1 and H_3. A sensitivity study enables to discuss the possibility of simultaneous identification of the parameters. This analysis takes into account the amplitude of the sensitivity to the parameters and checks the decorrelation conditions of the quantities. The study also allows to optimize the work frequential window according to the required objectives. It can finally lead to a reduction of the model if it proves that in the observation window certain parameters have a negligible role.

The functions H_1 and H_3 being complex functions of the frequency, we chose to study the sensitivities of the modules and the phases to the various parameters. The sensitivity functions of the module and the phase of one or the other of the two tested functions to parameter p_i will be defined by the relation:

$$X_{p_i}(f) = \frac{p_i \dfrac{\delta F(p_1, p_2, \cdots, p_n, f)}{\delta p_i}}{F(p_1, p_2, \cdots, p_n, f)}. \tag{9}$$

In the expression (9), F represents in turn the module of H_1, that of H_3, the phase of H_1 and that of H_3. There are in our case five parameters to test for each function because we can admit that the thickness of the sample is a known quantity. The sensitivities are defined by the ratio of the variations of the tested functions to relative variations of the parameters. To facilitate interpretation on a broad frequency band, these ratios are expressed as a percentage of the tested function. We have represented in Figures 3 and 4 the results relating to the frequency band ranging between 10^{-4} Hz and 10^{-1} Hz.

Figures 3a and 3b show the results obtained for the function H_1, whereas Figures 4a and 4b correspond to the

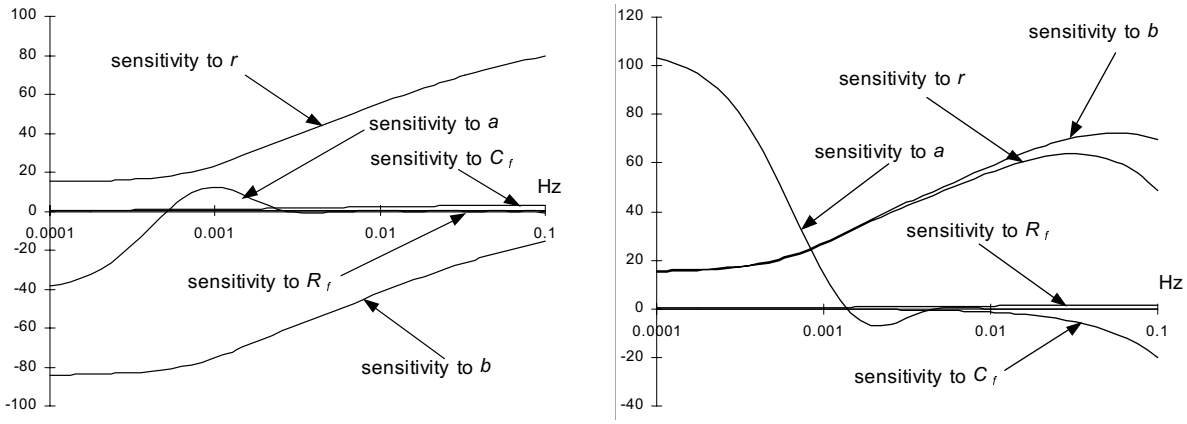

(a) (b)

Fig. 3. (a) Sensitivities of the module of H_1 to the parameters according to the frequency. (b) Sensitivities of the phase of H_1 to the parameters according to the frequency.

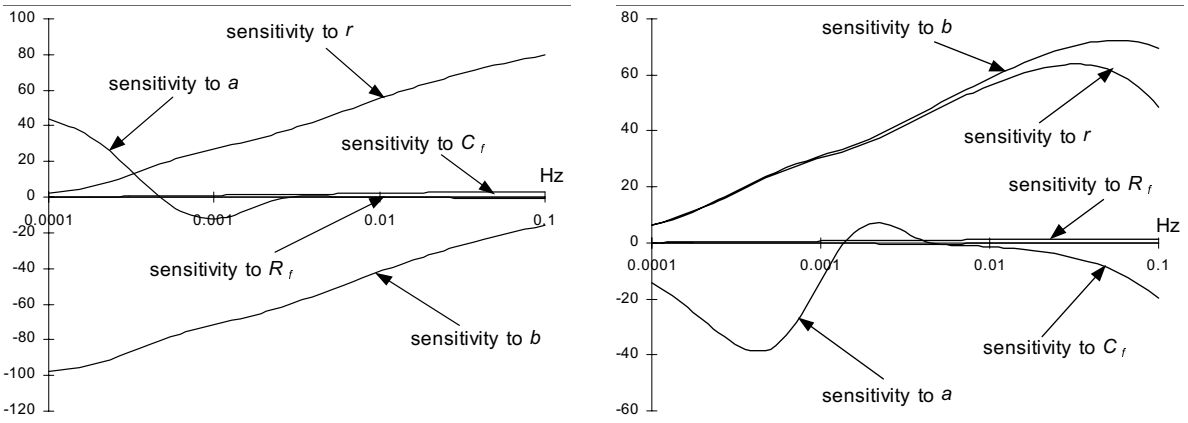

(a) (b)

Fig. 4. (a) Sensitivities of the module of H_3 to the parameters according to the frequency. (b) Sensitivities of the phase of H_3 to the parameters according to the frequency.

study of H_3. To carry out these calculations, some orders of quantity of the expected values of the parameters are injected into the model. They are mean values resulting from the literature or resulting from preliminary studies. The observation of the obtained sensitivity functions resulted in locating the study in a frequential window ranging between a few 10^{-4} Hz and a few 10^{-3} Hz. In this range, the sensitivities to the effusivity and diffusivity remain important and they are not correlated. We can however establish that the sensitivities of the two phases to the effusivity b and the contact resistance r have similar evolutions but the sensitivities of the modules are not correlated and allow a simultaneous identification. The two parameters are thus identifiable simultaneously. The sensitivities to resistances and capacities of the sensors being very low in the selected spectral band, these parameters could thus be neglected in this frequency band. Simulations carried out in parallel validated this conclusion. On the other hand, contact resistances (parameter r), must be taken into account. The reduced identification models include finally three unknown parameters that we have to identify simultaneously. One will thus retain for the study the following expressions of H_1 and H_3:

$$\begin{cases} H_1(f) = \dfrac{\cosh(X)(1+b\sqrt{\mathrm{j}\omega}) + \mathrm{j}rb^2\omega\sinh(X)}{2rb\sqrt{\mathrm{j}\omega}\cosh(X) + (1+\mathrm{j}rb^2\omega)\sinh(X)} \\ H_3(f) = \dfrac{\cosh(X)(1-b\sqrt{\mathrm{j}\omega}) + \mathrm{j}rb^2\omega\sinh(X)}{2rb\sqrt{\mathrm{j}\omega}\cosh(X) + (1+\mathrm{j}rb^2\omega)\sinh(X)} \end{cases} \tag{10}$$

where $X = \sqrt{(\mathrm{j}\omega/a)}\ell$.

In order to identify these parameters, an optimization of the setting of the ideal model on the experimental values is carried out independently for each function H. An iterative procedure of Levenberg-Marquardt [14] which enables to carry out an approximation of the data by a nonlinear model was used within this framework. This algorithm intends to minimize a merit function which is defined by the

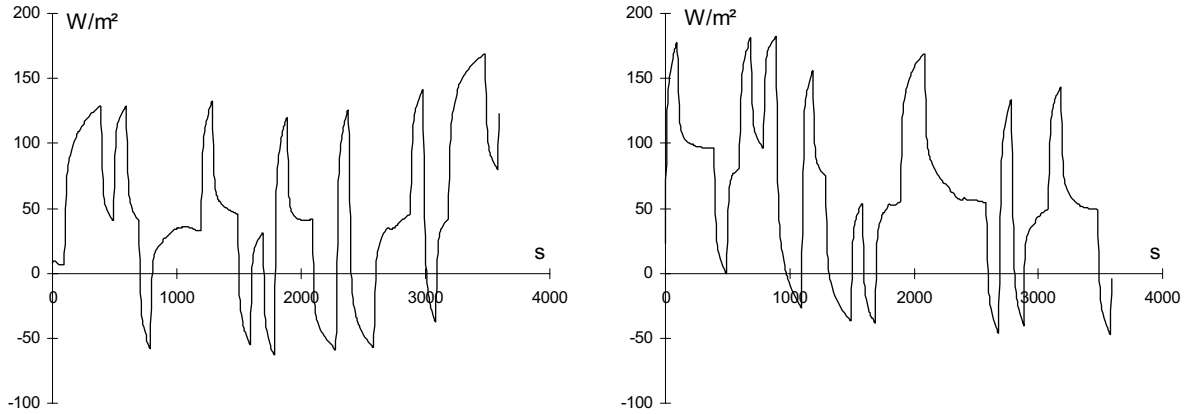

(a) (b)

Fig. 5. (a) Sum of the variations of measured flows according to time. (b) Difference of the variations of measured flows according to time.

following relation:

$$\chi^2(p_1,\ \cdots,\ p_n) = \sum_{i=1}^{k} \left(\frac{|H(i) - H_{\text{th}}(i, p_1,\ \cdots,\ p_n)|}{\sigma(i)} \right)^2 \quad (11)$$

with:

H_{th}: ideal model,
H: experimental curve to fit,
σ: standard deviation,
p_1, ..., p_n: grouping of parameters to be identified,
k: number of points retained for the study.

3 Experimental study

3.1 Description of the studied material

It concerns a foundry sand that does not contain fine element (< 80 μm). Its granulometric curve that only fills a small number of class dimensions, that implies a regular distribution of the grains forming each new sample. The samples are always brought into operation in the same way, that means by sinking of small layers, in order to make sure of the homogeneity of the medium.

These conditions allow us to consider the sample as symmetrical, and so to neglect the H_2 function, as we underlined in Section 2.1.

3.2 Measures

The method presented was applied to the characterization of this sand whose water content varies from 0 to 10%. We previously tried it out on reference material (plastics, glass), and obtained results did not deviate more than 2% from the expected values. In order to validate our measurements by studies of generalized impedances, we first carried out some characterizations of the tested samples by measurements of thermal conductivities and specific heat. The procedures relating to these traditional measurements are common in our laboratory and were already the subject of several works [8,15].

Our process demands that we carry out a simultaneous measurement of the flux density and temperature in the two access plans of the system. This is made possible thanks to the use of fluxmeters with tangential gradient in which a thermocouple is integrated. The two fluxmeters we used are identical. They have an active surface of 15×15 cm^2, and a guard ring guaranteeing the unidirectionality of the exchanges in the zone of measurement brings the sensor to a total surface of 25×25 cm^2. The fluxmeters deliver an electric tension proportional to the flow passing through them. The ratio of proportionality defines the sensitivity of the sensor which in our case is about a few tens of μV for 1 W/m^2. Their thickness is about 200 to 300 μm, which makes the sensors far from disturbing of the system at the slight frequencies, and then we can neglect them as we underlined in 2.2. It is however essential to integrate them into the model for high frequencies where they become increasingly disturbing as show the curves of sensitivities previously described.

The experimental device is represented Figure 1. The sample studied is placed between two fluxmeters which measure the flux densities and the temperatures on the two access faces of the system. The excitation is ensured on each face by a plane resistance whose supplying is controlled by a micro computer. The power of excitation delivered independently on each face describes a random pseudo binary signal. The whole is compressed between two plates whose role is to ensure a simple pressure of maintenance. Data acquisition is ensured by a scrutinizing multimeter of type Keithley 2000, controlled via a bus IEEE by a micro computer which stores the values.

As an example, the evolutions of the generalized magnitudes of flow and temperature obtained during one hour within the framework of a test carried out on a sample

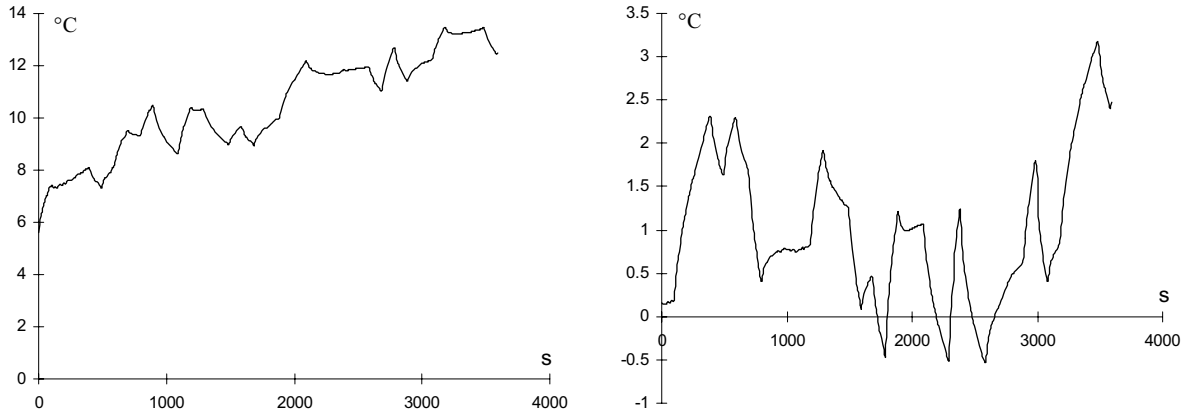

(a) (b)

Fig. 6. (a) Sum of the variations of measured temperatures with respect to a 16 °C constant temperature reference. (b) Difference of the variations of measured temperatures with respect to a 16 °C constant temperature reference.

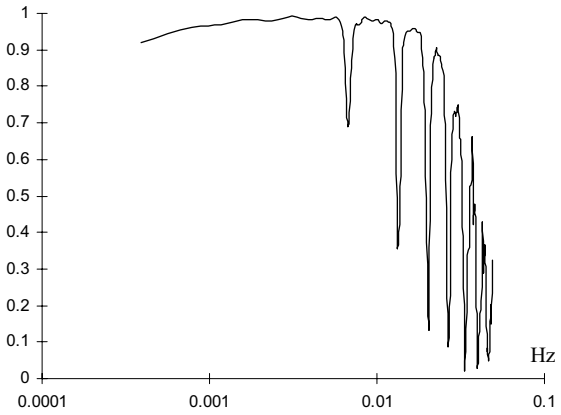

Fig. 7. Coherence function according to the frequency.

Table 1. Results obtained for a test on a 5% water content sand.

parameters	Study of H_1	Study of H_3	Preliminary test
a: $m^2\,s^{-1}$ $(\times 10^{-7})$	11.7	11.2	11.5
b: $J\,K^{-1}\,m^{-2}\,s^{-1/2}$	1660	1730	1650
λ: $W\,m^{-1}\,K^{-1}$	1.80	1.83	1.77

Table 2. Assessment of the results obtained for 3 water contents.

	Parameters:	0%	5%	10%
Preliminary tests	a: $m^2\,s^{-1}$ $(\times 10^{-7})$	2.8	11.5	11.1
	b: $J\,K^{-1}\,m^{-2}\,s^{-1/2}$	636	1650	1985
	λ: $W\,m^{-1}\,K^{-1}$	0.34	1.77	2.09
Study of H_1	a: $m^2\,s^{-1}$ $(\times 10^{-7})$	2.7	11.8	10.8
	average deviation: %	5.6	3.9	4.3
	b: $J\,K^{-1}\,m^{-2}\,s^{-1/2}$	610	1660	2010
	average deviation: %	4.2	1	1.2
	λ: $W\,m^{-1}\,K^{-1}$	0.32	1.8	2.1
	average deviation: %	5.7	1.9	2.0
Study of H_3	a: $m^2\,s^{-1}$$(\times 10^{-7})$	2.8	11.9	10.8
	average deviation: %	4.5	5.3	4.2
	b: $J\,K^{-1}\,m^{-2}\,s^{-1/2}$	664	1680	2020
	average deviation: %	4.9	2.1	2.2
	λ: $W\,m^{-1}\,K^{-1}$	0.35	1.83	2.1
	average deviation: %	5.6	2.5	3.1

with a water content of 5% are represented in Figures 5 and 6.

For this test, the supply voltages followed SBPA generated by shift registers of 5 cells and respective rates of clock of 100 and 150 seconds. Acquisition was carried out at a 10 seconds rate. We note on the evolution of $\Delta\theta$ that the deviation of the variations of measured temperature between the two faces does not exceed 3.5 °C [3]. Furthermore, the test mean temperature being near the atmosphere one, the phenomenon of change of inside phase is limited [9]. This results guarantee that the solicitation does not create migrations and does not disturb significantly hydrous balance.

The first phase of the proceeding consists in estimating the transfer functions (H_1 and H_3) from the method described into Section 2.1. From $\Sigma\phi$ and $\Delta\theta$, we obtained an estimate of H_1. The coherence function that is calculated at the same time enables to select the frequencies for which information is reliable. Figure 7 gives the function Γ for the treated test.

The coherence function shows that the intended frequency band is well-excited by the solicitations but that certain frequencies are too "disturbed" and must be moved aside. Function H_1 is represented Figure 8a, and $\Delta\phi$ and $\Sigma\theta$ make it possible to calculate H_3 whose evolution is represented Figure 8b.

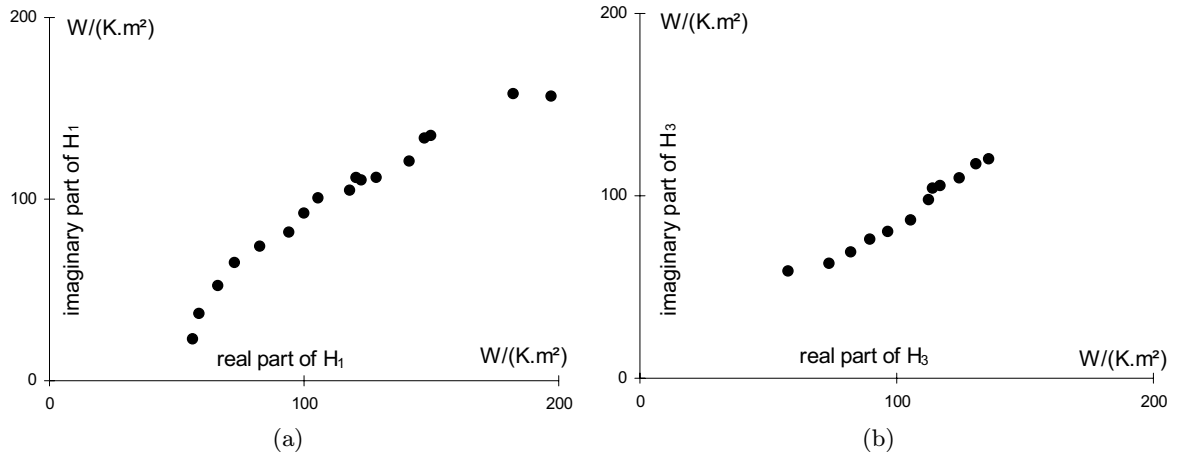

Fig. 8. (a) Function H_1: imaginary part according to the real part (diagram of Nyquist). (b) Function H_3: imaginary part according to the real part (diagram of Nyquist).

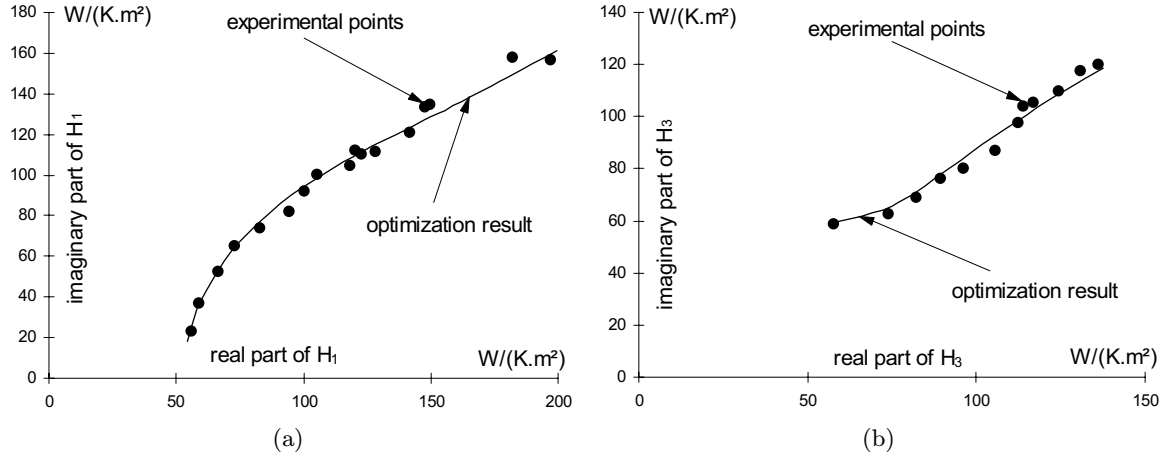

Fig. 9. (a) Function H_1: experimental and optimized curves. (b) Function H_3: experimental and optimized curves.

The second stage is the optimization procedure whose aim is to determine the grouping of parameters allowing to fit the experimental functions H_1 and H_3 by the theoretical curves, according to the criterion of optimization. Optimizations are carried out successively for the two functions and give for each test two estimates of the parameters.

Figure 9a represents the results of the approximation carried out for H_1. Figure 9b shows the result obtained for the same test for the function H_3. The values of the parameters resulting from this test are recorded in Table 1. We can verify an excellent agreement between, on one hand, the parameters resulting from the two functions H_1 and H_3, and on the other hand between these values and the preliminary test resulting from traditional measurements.

This process was adopted for water contents of 0, 5 and 10%, and for each water content 6 different tests were carried out. Table 2 shows the various average results as well as the average deviations compared to the values determined beforehand with the traditional way. We use these values as reference. About the three tested water contents, we note that the functions H_1 and H_3 gave access to precise estimates of the parameters a and b of material.

4 Conclusion

The results presented here show the interest of the concept of thermal impedance and the identification under random solicitations in order to characterize systems thermically. The developed procedure induced a very weak disturbance of the medium and thus minimizes the hydrous imbalance of material. The use of random solicitations and the associated frequential treatment make the method far from demanding as regard the limit conditions. The experimental methods are then very simple and use easy and inexpensive devices of measurement. The treatments allow us to be freed from the problems of the external thermal disturbances, and in situ measurements are completely possible although tests were carried out here in laboratory. Work

in progress intend to reduce the time of observation of the system by using estimate parametric methods of the transfer functions. The taking into account of a dissymmetry configuration is also studied.

References

1. W.H. Somerton, M. Mossahebi, Rev. Sci. Instr. **38**, 10 (1967).
2. D. Defer, E. Antczak, B. Duthoit, Meas. Sci. Technol **9**, 496 (1998).
3. M. Matsumoto, S. Hokoi, M. Yamamoto, Thermophys. Prop., 25 (1984).
4. P. Herin, P. Thery, Meas. Sci. Technol. **3**, 158 (1993).
5. A. Degiovanni, Heat Mass Trans. **31**, 553 (1988).
6. D. Defer, B. Duthoit, Rev. Gen. Therm. **395**, 633 (1994).
7. A.V. Oppenheim, C.T. Mullis, *Signals and systems* (Prentice-Hall, 1983).
8. B. Duthoit, D. Leclercq, P. Thry, J. Appl. Phys. **52**, 2 (1983).
9. S. Azizi, J.C. Batsale, C. Moyne, A. Degiovanni, Temp. High. Press. **21**, 383 (1989).
10. J.P. Bardon, in *Proceedings of the Colloque inter-universitaire Franco-Quebécois*, Toulouse, France, 1993, pp. 15–32.
11. J.S. Bendat, A.G.J. Piersol, *Measurements and Analysis of random Data* (Wiley, 1966).
12. J. Hladik, *Métrologie des propriétés thermophysiques des matériaux* (Masson, 1990).
13. J. Max, *Méthodes et techniques de traitement du signal et applications aux mesures physiques* (Masson, 1985), Vol. 2.
14. W. Press, B. Flannery, S. Teukolsky, W. Vetterling, *Numerical Recipes* (Cambridge University Press, 1986).
15. E. Antczak, Ph.D. thesis, Université d'Artois, 1996.